

---

*This copy is for your personal, non-commercial use only.*

---

**If you wish to distribute this article to others**, you can order high-quality copies for your colleagues, clients, or customers by [clicking here](#).

**Permission to republish or repurpose articles or portions of articles** can be obtained by following the guidelines [here](#).

**The following resources related to this article are available online at [www.sciencemag.org](http://www.sciencemag.org) (this information is current as of January 27, 2011 ):**

**Updated information and services**, including high-resolution figures, can be found in the online version of this article at:

<http://www.sciencemag.org/content/331/6016/411.full.html>

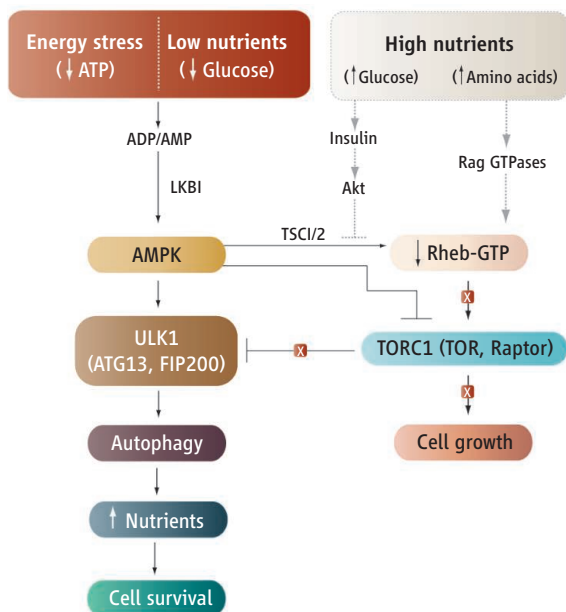
This article **cites 11 articles**, 5 of which can be accessed free:

<http://www.sciencemag.org/content/331/6016/411.full.html#ref-list-1>

This article appears in the following **subject collections**:

Chemistry

<http://www.sciencemag.org/cgi/collection/chemistry>



**Pathways linking nutrients and autophagy.** Under conditions of energy stress or glucose starvation, mammalian cells activate AMPK, which then phosphorylates and activates the ULK1 complex. AMPK also inactivates TORC1 by phosphorylating Raptor as well as by phosphorylating and activating TSC2 (converting Rheb to its inactive, GDP form). Signaling pathways that are blocked by AMPK activation under these conditions are marked with a cross. Glucose availability, acting in metazoans via insulin and Akt, activates TORC1 by phosphorylation and inactivation of TSC2. Amino acid availability activates TORC1 via the Rag GTPases. Thus, the ULK1 complex triggers autophagy during nutrient starvation and energy stress, whereas TORC1 inhibits autophagy and stimulates cell growth in the presence of nutrients and sufficient energy.

TORC1 (see the figure). AMPK inhibits TORC1 by phosphorylating its upstream regulator TSC2 (6) and the TORC1 subunit, Raptor (9). However, some of these mechanisms are not conserved in lower eukaryotes. Thus, there is no ortholog of TSC2 in *S. cerevisiae*, and although there is a Raptor ortholog (Kog1), because of a low degree of sequence conservation it is not clear whether the AMPK sites are conserved. Indeed, there is little current evidence that the yeast AMPK ortholog (the SNF1 complex) acts upstream of TOR, although there is evidence that it regulates autophagy. In *snf1* mutants the increase in autophagy induced when cells enter stationary phase due to glucose depletion is defective, whereas both *ATG1* and *ATG13* suppress the phenotype of low glycogen accumulation observed during stationary phase (13). Thus, the “belt” of activation of ULK1 (Atg1) by AMPK (SNF1) may have evolved early, whereas the “braces” of inhibition of TORC1 by AMPK may have arisen later. One can only speculate as to why this might have happened, although the role of the AMPK complex itself also

appears to have changed. In yeast, the SNF1 complex is probably mainly concerned with the response to glucose starvation, but for mammalian cells the ability of AMPK to sense energy status may have become more important. Perhaps inhibition of TORC1 by AMPK evolved as a mechanism to ensure that autophagy remains active and growth repressed during energy stress, even though amino acids are available.

#### References and Notes

1. S. L. Clark Jr., *J. Biophys. Biochem. Cytol.* **3**, 349 (1957).
2. C. de Duve, R. Wattiaux, *Annu. Rev. Physiol.* **28**, 435 (1966).
3. D. F. Egan *et al.*, *Science* **331**, 456 (2011); 10.1126/science.1196371.
4. M. Tsukada, Y. Ohsumi, *FEBS Lett.* **333**, 169 (1993).
5. Y. Sancak *et al.*, *Science* **320**, 1496 (2008).
6. K. Inoki, T. Zhu, K. L. Guan, *Cell* **115**, 577 (2003).
7. D. M. Gwinn *et al.*, *Mol. Cell* **30**, 214 (2008).
8. B. Xiao *et al.*, *Nature* **449**, 496 (2007).
9. W. A. Wilson, S. A. Hawley, D. G. Hardie, *Curr. Biol.* **6**, 1426 (1996).
10. J. W. Scott, D. G. Norman, S. A. Hawley, L. Kontogiannis, D. G. Hardie, *J. Mol. Biol.* **317**, 309 (2002).
11. C. Behrends, M. E. Sowa, S. P. Gygi, J. W. Harper, *Nature* **466**, 68 (2010).
12. In an alignment by this author, correspondence of Ser<sup>555</sup> with Thr<sup>484</sup> was not convincing, while Thr<sup>532</sup> in *C. elegans* aligned with Ser<sup>537</sup> rather than Thr<sup>574</sup>.
13. Z. Wang, W. A. Wilson, M. A. Fujino, P. J. Roach, *Mol. Cell. Biol.* **21**, 5742 (2001).

10.1126/science.1201691

in cells expressing the 4A mutant, either under normal culture conditions or during nutrient starvation. Egan *et al.* claim that the Ser<sup>555</sup> and Thr<sup>574</sup> sites are conserved in the nematode *Caenorhabditis elegans* ortholog Unc-51, although this can be debated (12). They do provide evidence that the *C. elegans* ortholog of AMPK (Aak-2) triggers autophagy, although the role of phosphorylation of Unc-51 was not addressed.

Although further work is required to delineate the roles of the individual phosphorylation sites, the findings of Egan *et al.* suggest that the AMPK signaling pathway uses a “belt and braces” approach to activate autophagy in mammals, using both phosphorylation of ULK1 and inhibition of

the AMPK sites are conserved. Indeed, there is little current evidence that the yeast AMPK ortholog (the SNF1 complex) acts upstream of TOR, although there is evidence that it regulates autophagy. In *snf1* mutants the increase in autophagy induced when cells enter stationary phase due to glucose depletion is defective, whereas both *ATG1* and *ATG13* suppress the phenotype of low glycogen accumulation observed during stationary phase (13). Thus, the “belt” of activation of ULK1 (Atg1) by AMPK (SNF1) may have evolved early, whereas the “braces” of inhibition of TORC1 by AMPK may have arisen later. One can only speculate as to why this might have happened, although the role of the AMPK complex itself also

## CHEMISTRY

# Chemical Kinetics Under Test

Millard H. Alexander

The dependence of reaction rates on the isotopic identity of the reactants and products, called the “kinetic isotope effect” (1–3), is a manifestation of the role quantum zero-point energy plays in chemical kinetics and is a consequence of the Born-Oppenheimer (BO) separation of electronic and nuclear motion in molecules (4, 5). On page 448 of this issue, Fleming

*et al.* (6) use muon chemistry to probe the range of nuclear masses over which this approximation is valid for the chemical reaction  $H + H_2 \rightarrow H_2 + H$  (7).

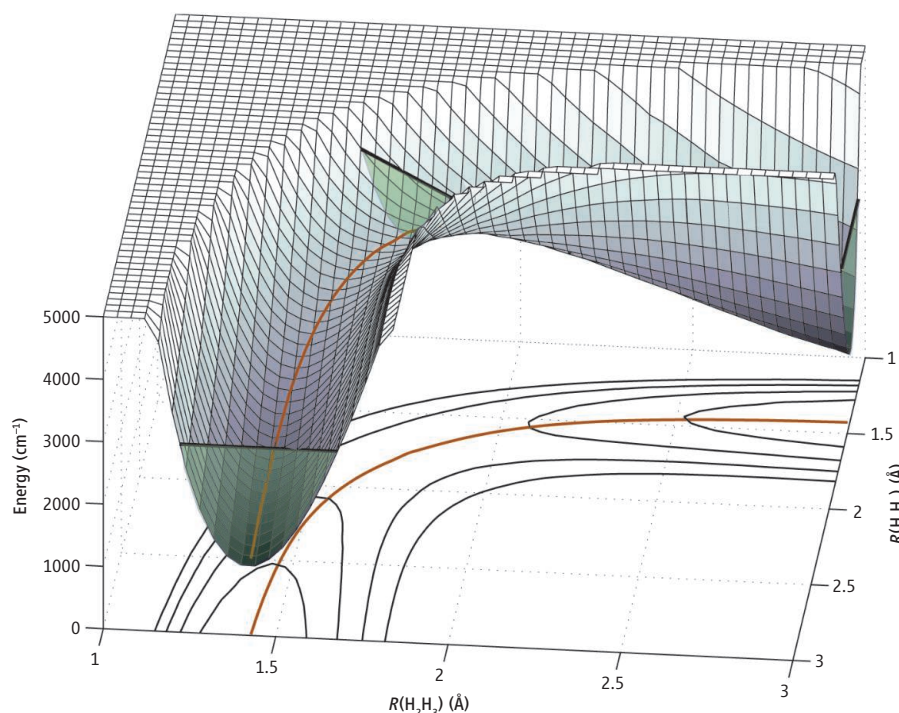
The BO approximation makes possible the practical application of quantum mechanics to all of molecular science. As the arrangement of the nuclei changes, the BO approximation postulates that the electrons will remain in a particular quantum state. The practical implication is that any molecule, consisting of a number of nuclei and, usually, a larger number of electrons, can be treated

A wide range of hydrogen and helium isotopes serve as a fundamental test of isotope effects and tunneling in chemical reactions.

quantum mechanically in two stages. First, for a given nuclear arrangement, one determines the energy of the electrons, usually in their ground electronic state. The gradient of this electronic energy (along with the electrostatic repulsion between the nuclei) then determines the forces on the nuclei. This two-stage separation enables the understanding of molecular spectroscopy as well as the simulation of the molecular dynamics in systems ranging from the simple to the complex.

One direct consequence of the BO approximation is the understanding of an

Department of Chemistry and Biochemistry and Institute for Physical Science and Technology, University of Maryland, College Park, MD 20742–2021, USA. E-mail: mha@umd.edu



**Mapping out a reaction.** Surface mesh plot of the potential energy surface for the collinear  $\text{H}_1 + \text{H}_2\text{H}_3 \rightarrow \text{H}_1\text{H}_2 + \text{H}_3$  reaction as a function of the two bond distances,  $R$ , superimposed on a conventional contour plot of the potential energy surface. The minimum-energy reaction path is indicated by the solid orange line. The zero-point energy in the reactant and product arrangements, and at the barrier, is indicated by straight black lines. The three corresponding green slices indicate the range of coordinate space made classically accessible by zero-point energy.

important quantum effect in chemical kinetics: the kinetic isotope effect (*I–3*). Consider the simplest diatomic molecule  $\text{H}_2$  and its isotopomer HD (hydrogen deuteride). Within the BO approximation, both  $\text{H}_2$  and HD have the same electronic Hamiltonian and, thus, the same potential energy curves. However, because their nuclear reduced masses are so different [0.50 atomic mass units (amu) for  $\text{H}_2$  and 0.66 amu for HD], the vibrational spacing differs dramatically. In particular, the quantum zero-point energy of  $\text{H}_2$  is 33% larger than that of HD.

Especially in the case of H transfer and exchange, the dependence of zero-point energy on the isotopic identity of the reactants and/or products in a chemical reaction can lead to large differences in equilibrium constants and chemical reaction rate constants (*I–3*). The isotopic variation of the zero-point energy will affect not only the reaction exothermicity but also the height of the transition state—the activation energy. The magnitude of the rate constant is proportional to the density of vibration-rotation states of the reaction complex at the transition state, which also depends on the isotopic masses (*I*).

A subtle consequence of differing isotopic masses on chemical reaction rates can be

seen in terms of the potential energy surface for the  $\text{H} + \text{H}_2$  reaction (see the figure). The appreciable zero-point motion of the light H atom implies that the reaction occurs not just along the reaction path, which is the minimum-energy pathway depicted in the figure, but also over a sizable region of configuration space around this minimum path, as indicated by the green slices. Isotopic substitution will control the width of the slice of the potential energy surfaces sampled during the reaction.

Fleming *et al.* report the study of  $\text{H} + \text{H}_2$  reactivity over the widest possible range of isotopic masses. First, they have succeeded in replacing the H atom with muonium (an electron orbiting a positive muon,  $\mu^+$ ). Within the BO approximation, this behaves as a very light H atom with a mass of only 0.11 amu. On the other end of the scale, they have replaced one of the electrons in the  $^4\text{He}$  atom with a negative muon,  $\mu^-$ . Because  $\mu^-$  is 207 times heavier than the electron, it orbits the He nucleus at a very close range, effectively screening one of the protons. Thus, the  $^4\text{He}\mu$  system behaves chemically as a very heavy H atom with mass of 4.1 amu.

The rate constants from these unique experiments, combining accelerator physics

and chemical kinetics, are compared with full quantum-mechanical reactive-scattering calculations (*8*), based on a very sophisticated BO  $\text{H}_3$  potential energy surface (*9*), and with the result of a variational extension of transition state theory (*10*), in its latest form (*11*). Excellent agreement is found with experiment over the entire range, in which the mass of the H atom is varied from 0.11 amu, through 1 amu (the mass of the normal H atom), and then to 4.1 amu. The tests reported by Fleming *et al.* over a large range of isotopic masses thus verifies the BO separation of electronic and nuclear motion in the paradigm  $\text{H} + \text{H}_2$  reaction. Further, the comparison between the exact quantum treatment of the nuclear dynamics and (modified) transition state theory has shown that the latter accurately describes the subtle variation of chemical reactivity with the isotopic mass of the reactant, at least in the  $\text{H} + \text{H}_2$  reaction.

The quantitative agreement between theory and experiment seen by Fleming *et al.* confirms our ability to predict with high accuracy the fine details of potential energy surfaces for small triatomic reactions and to model the details of the reaction dynamics.

However, a breakdown in any approximation is always possible. Recent work (*12, 13*) has delimited the small, but measurable, BO breakdown in the simplest chemical reaction beyond  $\text{H} + \text{H}_2$ , namely  $\text{F} + \text{H}_2 \rightarrow \text{FH} + \text{H}$  and its analog  $\text{Cl} + \text{H}_2 \rightarrow \text{ClH} + \text{H}$ . One wonders whether it would be possible to find a triatomic reaction with a barrier in which the dependence of the rate constants (or, in more detail, the cross sections) on the isotopic mass of the reactants deviates from the predictions of transition state theory.

#### References and Notes

1. I. W. M. Smith, *Kinetics and Dynamics of Elementary Gas Reactions* (Butterworths, London, 1980).
2. R. E. Weston Jr., *Science* **158**, 332 (1967).
3. J. Bigeleisen, M. G. Mayer, *J. Chem. Phys.* **15**, 261 (1947).
4. M. Born, R. Oppenheimer, *Ann. Phys.* **389**, 457 (1927).
5. [http://en.wikipedia.org/wiki/Born–Oppenheimer\\_approximation](http://en.wikipedia.org/wiki/Born–Oppenheimer_approximation).
6. D. G. Fleming *et al.*, *Science* **331**, 448 (2011).
7. J. V. Michael, J. R. Fisher, J. M. Bowman, Q. Sun, *Science* **249**, 269 (1990).
8. Y. Sun, D. J. Kouri, D. G. Truhlar, D. W. Schwenke, *Phys. Rev. A* **41**, 4857 (1990).
9. S. L. Mielke, B. C. Garrett, K. A. Peterson, *J. Chem. Phys.* **116**, 4142 (2002).
10. D. G. Truhlar, B. C. Garrett, *Acc. Chem. Res.* **13**, 440 (1980).
11. B. C. Garrett, D. G. Truhlar, R. S. Grev, A. W. Magnuson, *J. Phys. Chem.* **84**, 1730 (1980).
12. L. Che *et al.*, *Science* **317**, 1061 (2007).
13. X. Wang *et al.*, *Science* **322**, 573 (2008).
14. Supported by the U.S. National Science Foundation (grant CHE-0848110) and by the U.S. Department of Energy (grant DES0002323).